AD-A158 417

DNA-TR-84-288-V3

THEORY SUPPORT OF PULSED POWER EXPERIMENTS
Volume III—E-Beam Chamber Design

S-CUBED
A Division of Maxwell Laboratories, Inc.
P.O. Box 1620
La Jolla, CA 92038-1620

1 July 1984

Technical Report

CONTRACT No. DNA 001-79-C-0027

DTIC FILE COPY

DTIC
ELECTE
AUG 2 8 1985

B

Prepared for
Director
DEFENSE NUCLEAR AGENCY
Washington, DC 20305-1000

85 06 14 034

REPORT DOCUMENTATION PAGE

1a REPORT SECURITY CLASSIFICATION		1b RESTRICTIVE MARKINGS			
UNCLASSIFIED					
2a SECURITY CLASSIFICATION AUTHORITY		3 DISTRIBUTION AVAILABILITY OF REPORT			
		Approved for public release; distribution is unlimited.			
2b DECLASSIFICATION DOWNGRADING SCHEDULE					
N/A since UNCLASSIFIED					
4 PERFORMING ORGANIZATION REPORT NUMBER(S)		5 MONITORING ORGANIZATION REPORT NUMBER(S)			
SSS-R-84-6709-III		DNA-TR-84-288-V3			
6a NAME OF PERFORMING ORGANIZATION	6b OFFICE SYMBOL (If applicable)	7a NAME OF MONITORING ORGANIZATION			
S-CUBED, A Division of Maxwell Laboratories, Inc.		Director Defense Nuclear Agency			
6c ADDRESS (City, State, and ZIP Code)		7b ADDRESS (City, State, and ZIP Code)			
P.O. Box 1620 La Jolla, CA 92038-1620		Washington, DC 20305-1000			
8a NAME OF FUNDING SPONSORING ORGANIZATION	8b OFFICE SYMBOL (If applicable)	9 PROCUREMENT INSTRUMENT IDENTIFICATION NUMBER			
		DNA 001-79-C-0027			
8c ADDRESS (City, State, and ZIP Code)		10 SOURCE OF FUNDING NUMBERS			
		PROGRAM ELEMENT NO	PROJECT NO	TASK NO	WORK UNIT ACCESSION NO
		62715H	T99QAXL	A	DH005792

11 TITLE (Include Security Classification)
THEORY SUPPORT OF PULSED POWER EXPERIMENTS
Volume III—E-Beam Chamber Design

12 PERSONAL AUTHOR(S)
A. Wilson, D.E. Parks, E.M. Waisman, M.C. Friedman, P.G. Steen, M. Chapman

13a TYPE OF REPORT	13b TIME COVERED	14 DATE OF REPORT Year Month, Day	15 PAGE COUNT
Technical	FROM 781115 TO 820930	1984 July 1	28

16 SUPPLEMENTARY NOTATION
This work was sponsored by the Defense Nuclear Agency under RDT&E RMSS Code
B323082466 T99QAXLA00022 H2590D.

17	COSATI CODES		18 SUBJECT TERMS (Continue on reverse if necessary and identify by block number)
FIELD	GROUP	SUB-GROUP	X-Ray Simulators
20	7		Power Flow
10	2		BACCARAT

19 ABSTRACT (Continue on reverse if necessary and identify by block number)

The progress made in understanding the physics of x-ray simulators is presented. The work includes sections on diode power flow, plasma stability and dynamics, e-beam test chambers and the DNA BACCARAT program.

20 DISTRIBUTION AVAILABILITY OF ABSTRACT	21 ABSTRACT SECURITY CLASSIFICATION	
☐ UNCLASSIFIED UNLIMITED ☒ SAME AS RPT ☐ DTIC USERS	UNCLASSIFIED	
22a NAME OF RESPONSIBLE INDIVIDUAL	22b TELEPHONE (Include Area Code)	22c OFFICE SYMBOL
Betty L. Fox	(202)325-7042	DNA/STTI

DD FORM 1473, 84 MAR

83 APR edition may be used until exhausted
All other editions are obsolete

TABLE OF CONTENTS

LIST OF ILLUSTRATIONS

LIST OF ILLUSTRATIONS (CONCLUDED)

2

SECTION 1
E-BEAM TEST CHAMBER DESIGN

In an SXTF-related effort, the charging of a satellite by multiple electron beams in a test chamber was examined (Appendix A1). The NASCAP 3-D computer model was used to simulate the dynamic charging of the test object for up to ten minutes. The effects of the earth's magnetic field were relatively small in the SXTF test chamber because of its relatively modest dimensions. However, the effects of enhanced backscatter and secondary electrons lead to substantial differential charging and electric field reversal.

Accession For

NTIS GRA&I	☑	
DTIC TAB	☐	
Unannounced	☐	
Justification		

By
Distribution/
Availability Codes

Dist	Avail and/or Special
A-1	

APPENDIX
MULTIGUN TEST TANK SIMULATION WITH MAGNETIC FIELD
(TOPICAL REPORT SSS-R-81-5028, JUNE 1981)

A-1   INTRODUCTION

The simulation of spacecraft charging in ground based
facilities is of importance both for the study of electro-
static discharges and for precharge enhanced SGEMP. Since
it is not possible to recreate the high temperature, low
density plasmas of a magnetospheric substorm experimentally,
the charging environment usually consists of several electron
guns which spray a test satellite with charged particles.
Important questions are what charging results from these
guns and how does it relate to natural spacecraft charging.

In order to answer these questions we have developed
a tank multigun capability for the NASA Charging Analyzer
Program. NASCAP has already been shown valid for predicting
satellite potentials in space and is now able to model up
to ten multi-energy electron or ion guns, each of which
may arbitrarily be located and point in an arbitrary direction.
Also, the angular width of each beam may be specified.
One feature of the NASCAP algorithms is that they account
for finite Larmor radius effects on the charged particle
beams. The new multigun facility in NASCAP is both flexible
and fast running.

We have used NASCAP to model the electron irradiation
of SCATSAT, a test object built to examine the charging
and electromagnetic response of the SCATHA satellite. Experi-
ments are presently being performed at NASA/LeRC during
which four 6 keV electron guns are directed at SCATSAT.
In a dark isotropic space environment this object would
have charged relatively uniformly. However, during the

laboratory experiments there developed differential potentials of over a thousand volts which led to spontaneous discharges. The NASCAP calculations presented here show clearly what led to the differential charging in these experiments: Electrons obliquely incident on surfaces have high secondary electron yields. This new NASCAP capability may be used to explore questions of optimal beam placement, number and species of particle sources, and photoeffects for optimal design of laboratory simulations of spacecraft charging.

A-2   RESULTS

The geometry considered is a one meter electrically
floating octagonal object in a 3.2 m cubical tank. The
object was covered with 0.005 inch thick kapton, and was
illuminated by four monoenergetic flood guns. Each gun
emitted 5 mA of electrons distributed as $\cos(\pi\theta/2\theta_o)$, where
θ is the angle from the gun axis and θ_o was set to 30 degrees.
The magnetic field, when applied, was parallel to two of
the gun axes and normal to the other two.
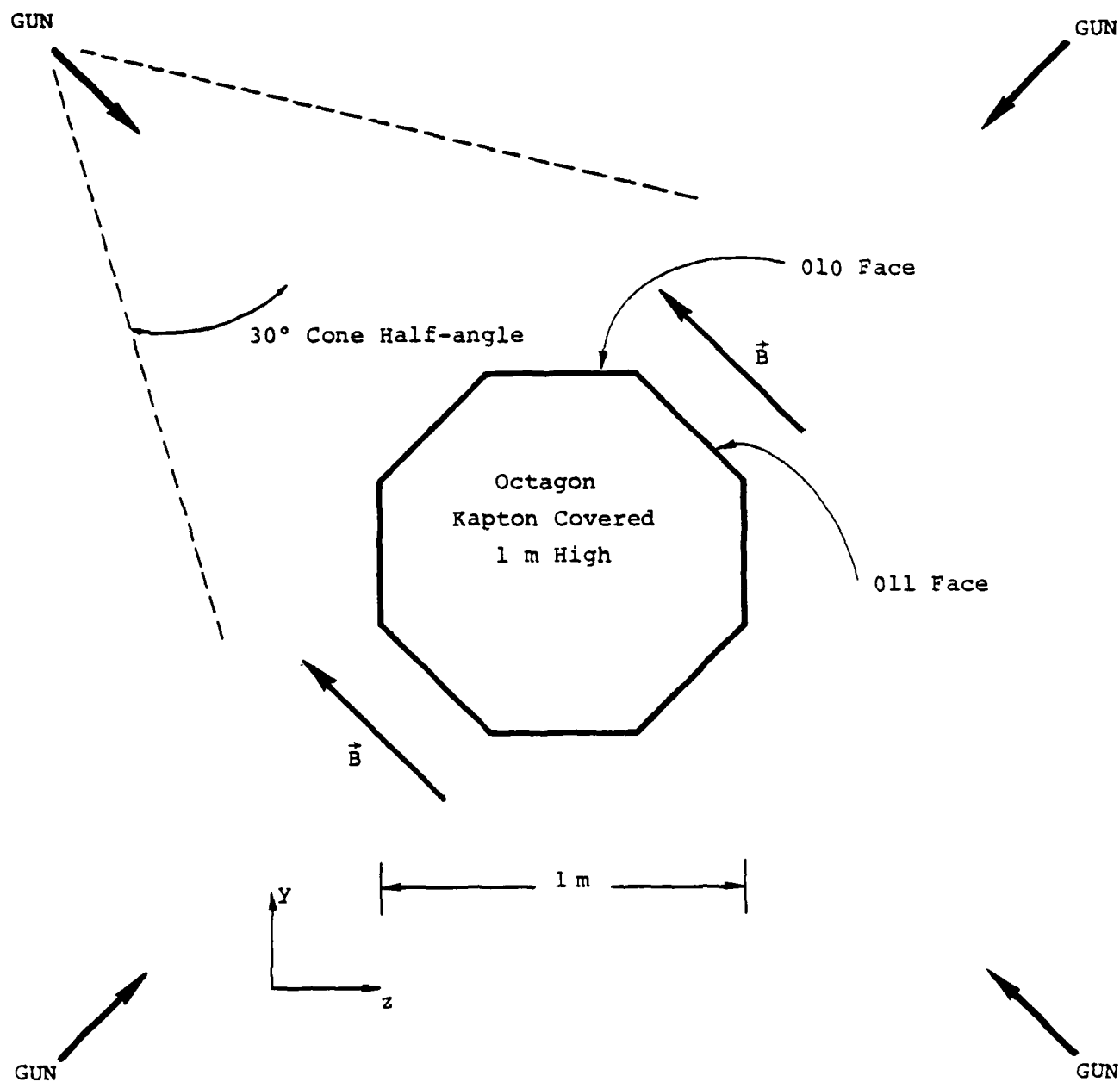
GUN

GUN

010 Face

$\vec{B}$

30° Cone Half-angle

Octagon
Kapton Covered
1 m High

011 Face

$\vec{B}$

1 m

Y

z

GUN

GUN

Figure A-1. Geometry of a one meter electrically floating
octagonal object in a 3.2 m cubical tank.

8

|	10 keV	10 keV	6 keV
Beam Energy			
$\vec{B}$ (gauss)	0	(0.,-.3,.3)	(0.,-.3,.3)
Cyclotron Radius	7.9 m	7.9 m	6.2 m
Distance from Gun to Nearest Surface	1.9 m	1.9 m	1.9 m
Peak Potential: 0$\bar{1}$1 Surface	-8540	-8540	-4790
360 sec at x =	0	0	0
Peak Potential: 011 Surface	-8540	-8540	-4700
360 sec at x =	0	0.10	0
Peak Potential: 010 Surface	-6260	-6340	-2920
360 sec at x =	0	0.35	0.45
Minimum Potential: 010 Surface	-6200	-5950	-2580
360 sec at x =	±0.45	-0.45	-0.45
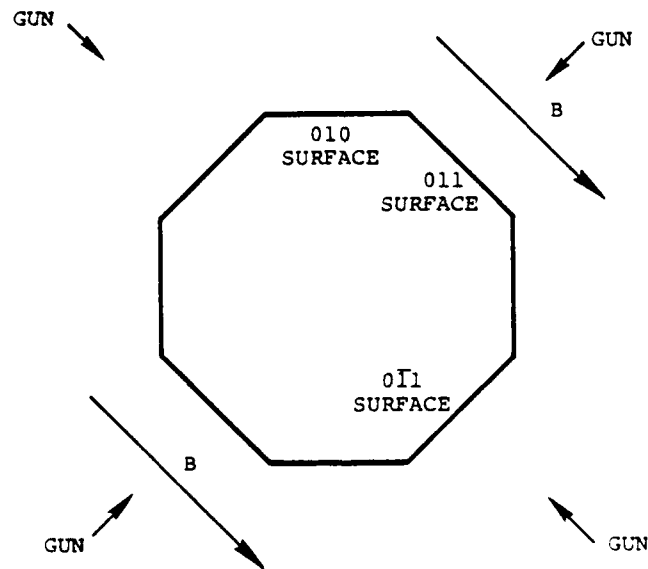
Figure A-2. The three simulations performed were 10 keV beams with and without magnetic field, and 6 keV beams with magnetic field. In all cases, differential charging in excess of 2 kV developed within six minutes. As the gun-object distance was a modest fraction of a cyclotron radius, magnetic field effects, though definitely noticeable, were correspondingly modest.
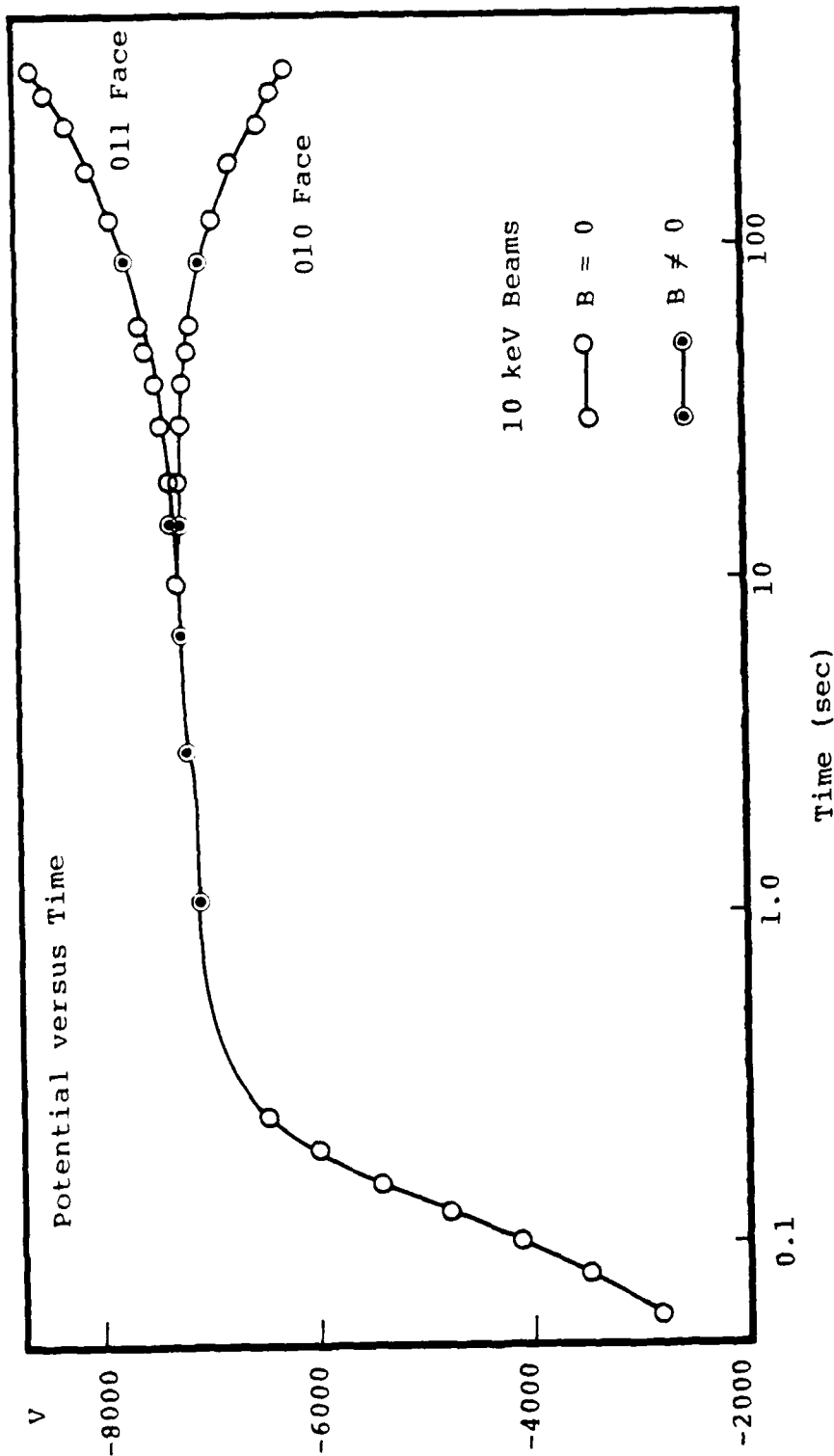
Figure A-3.   Potential for two cells near the spacecraft belly, exposed to 10 keV electrons. The object charges uniformly to about -7200 V in about one second. Over the next several minutes the surfaces receiving normally incident electrons continue to charge negatively, while those receiving obliquely incident electrons charge positively due to increased secondary emission. With exposure to 6 kV beams, the plateau voltage was -3600 volts. Magnetic fields, for the strength and geometry considered here, do not greatly alter this behavior.

10

Aerospace Corp
     ATTN: Library Acquisition M1/199
     ATTN: V. Josephson
     ATTN: S. Bower

BDM Corp
     ATTN: L. Shaeffer
     ATTN: L. Hoeft

BDM Corp
     ATTN: Corporate Lib

Berkeley Rsch Associates, Inc
     ATTN: E. Alcaraz

Boeing Co
     ATTN: Aerospace Library

Dikewood Corp
     ATTN: Tech Lib for D. Pirio

EG&G Wash Analytical Svc Ctr, Inc
     ATTN: Library

EOS Technologies, Inc
     ATTN: B. Gabbard

General Electric Co
     ATTN: J. Peden
     ATTN: H. O'Donnell

IRT Corp
     ATTN: R. Mertz
     ATTN: N. Rudie

JAYCOR
     ATTN: E. Wenaas

JAYCOR
     ATTN: C. Rogers

JAYCOR
     ATTN: R. Sullivan
     ATTN: E. Alcaraz

Kaman Sciences Corp
     ATTN: S. Face

Kaman Sciences Corp
     ATTN: E. Conrad

Kaman Tempo
     ATTN: DASIAC

Kaman Tempo
     ATTN: DASIAC

Lockheed Missiles & Space Co, Inc
     ATTN: S. Taimuty

Lockheed Missiles & Space Co, Inc
     ATTN: L. Chase

Martin Marietta Denver Aerospace
     ATTN: M. Peel

Maxwell Labs, Inc
     ATTN: A. Kolb
     ATTN: D. Tanimoto
     ATTN: A. Miller
     ATTN: O. Cole

McDonnell Douglas Corp
     ATTN: S. Schneider

Mission Research Corp
     ATTN: C. Longmire

Mission Research Corp
     ATTN: B. Godfrey

Mission Research Corp
     ATTN: V. Van Lint

Pacific-Sierra Research Corp
     ATTN: H. Brode, Chairman SAGE
     ATTN: L. Schlessinger

Physics International Co
     ATTN: C. Stallings
     ATTN: C. Gilman
     ATTN: G. Frazier

Pulse Sciences, Inc
     ATTN: I. Smith
     ATTN: P. Spence
     ATTN: S. Putnom

R&D Associates
     ATTN: C. Knowles
     ATTN: A. Latter
     ATTN: P. Haas

R&D Associates
     ATTN: P. Turchi

Rand Corp
     ATTN: P. Davis

Rand Corp
     ATTN: B. Bennett

S-CUBED
     ATTN: A. Wilson
     ATTN: D. Parks
     ATTN: E. Waisman
     ATTN: M. Friedman
     ATTN: P. Steen
     ATTN: M. Chapman

Science Applications Intl Corp
     ATTN: K. Sites

Science Applications Intl Corp
     ATTN: W. Chadsey
     ATTN: M. Schmidt

TRW Electronics & Defense Sector
     ATTN: D. Kingsland
     ATTN: D. Clement
     ATTN: Tech Info Ctr

DISTRIBUTION LIST

DEPARTMENT OF DEFENSE

Asst to the Secy of Defense, Atomic Energy
 ATTN: Exec Asst
 ATTN: J. Rubell

Defense Intelligence Agency
 ATTN: DT-1B, R. Rubenstein

Defense Nuclear Agency
 ATTN: RAAE
 ATTN: STNA
 ATTN: RAEE
2 cy ATTN: RAEV
4 cy ATTN: STTI/CA

Defense Tech Info Ctr
12 cy ATTN: DD

Field Command/DNA, Det 1
Lawrence Livermore National Lab
 ATTN: FC-1

Field Command, Defense Nuclear Agency
 ATTN: FCPR
 ATTN: FCTT
 ATTN: FCTXE
 ATTN: FCTT, W. Summa

Under Secy of Def for Rsch & Engrg
 ATTN: Strat & Space Sys (OS)

DEPARTMENT OF THE ARMY

Harry Diamond Laboratories
 ATTN: DELHD-NW-P, 20240
 ATTN: DELHD-NW-RA, 22100
 ATTN: DELHD-NW-RI, Kervis, 22900
 ATTN: DELHD-TA-L, 81100, Tech Lib

US Army Nuclear & Chemical Agency
 ATTN: Library

US Army Test and Evaluation Comd
 ATTN: DRSTE-CT-C

USA Missile Command
 ATTN: Documents Section

DEPARTMENT OF THE NAVY

Naval Research Laboratory
 ATTN: Code 2000, J. Brown
 ATTN: Code 4720, J. Davis
 ATTN: Code 4700, S. Ossakow
 ATTN: Code 4770, G. Cooperstein
 ATTN: Code 4701, I. Vitokovitsky

Naval Surface Weapons Ctr
 ATTN: Code R40
 ATTN: Code F31
 ATTN: Code F34

Naval Weapons Ctr
 ATTN: Code 343, FKA6A2, Tech Svcs

DEPARTMENT OF THE AIR FORCE

Air Force Weapons Laboratory
 ATTN: CA
 ATTN: NT
 ATTN: SUL
 ATTN: NTYP

Ballistic Missile Office
 ATTN: ENSN

Deputy Chief of Staff, Research, Dev, & Acq
 ATTN: AF/RDQI

Space Division
 ATTN: XR, Plans
 ATTN: YEZ
 ATTN: YGJ
 ATTN: YKF
 ATTN: YKM
 ATTN: YKS, P. Stadler
 ATTN: YNV

Strategic Air Command
 ATTN: DOTP
 ATTN: XPFS

DEPARTMENT OF ENERGY

Office of Military Application, GTN
 ATTN: Ofc of Inert Fusion, T. Godlove
 ATTN: Ofc of Inert Fusion, C. Hilland
 ATTN: Ofc of Inert Fusion, S. Kahalas

OTHER GOVERNMENT AGENCY

Central Intelligence Agency
 ATTN: OSWR/NED

DEPARTMENT OF ENERGY CONTRACTORS

University of California
Lawrence Livermore National Lab
 ATTN: L-47, L. Wouters
 ATTN: L-153
 ATTN: L-13, D. Meeker
 ATTN: L-545, J. Nuckolls
 ATTN: Technical Info Dept Library
 ATTN: W. Pickles, L-401

Los Alamos National Laboratory
 ATTN: MS222, J. Brownell

Sandia National Laboratories
 ATTN: Tech Lib 3141
 ATTN: G. Yonas
 ATTN: G. Kuswa, Org 5240
 ATTN: M. Clauser, Org 5241
 ATTN: Org 9336, D. Allen
 ATTN: J. Powell

DEPARTMENT OF DEFENSE CONTRACTORS

Advanced Research & Applications Corp
 ATTN: R. Armistead

NASCAP now has the computational capability for modeling this type of experiment. This capability should be used for facility design, experimental design, and experiment analysis.

A-3 CONCLUSIONS

Experimental simulation of spacecraft charging in
a three-dimensional, multigun facility is an extremely complex
process. Even for the relatively simple geometry considered
in this report, the combined effects of beam spreading,
angular dependence of emission coefficient, magnetic deflec-
tion, and potential barrier formation produce effects not
anticipated in the experimental design, and require three-
dimensional analysis. The added complexities of realistic
spacecraft and more elaborate simulation facilities further
underline the need for a computational modeling capability.

The magnetic field effects seen in these calculations,
though visible, are surprisingly small. This may not be
the case in a facility which is an order of magnitude larger,
unless the earth's magnetic field is substantially attenuated.
However, the reduction by a factor of three or more is
probably sufficient, and reduction by an order of magnitude
not necessary.

The most dramatic effects seen here are those caused
by the anisotropy of the beam environment. When we take
into account the enhanced backscatter and secondary electron
production for obliquely incident electrons, we see substan-
tial differential charging and large regions of electric
field reversal. These conditions will lead to surface flash-
overs and greatly enhanced SGEMP. While here this charge
state is attributable to beam anisotropy, the discharges
observed experimentally are similar to those seen on board
spacecraft.

POTENTIAL CONTOURS ALONG THE Y-Z PLANE OF X - 9

ZMIN - -4.9958+003   ZMAX - -1.1489+003   DZ - 2.0000+002
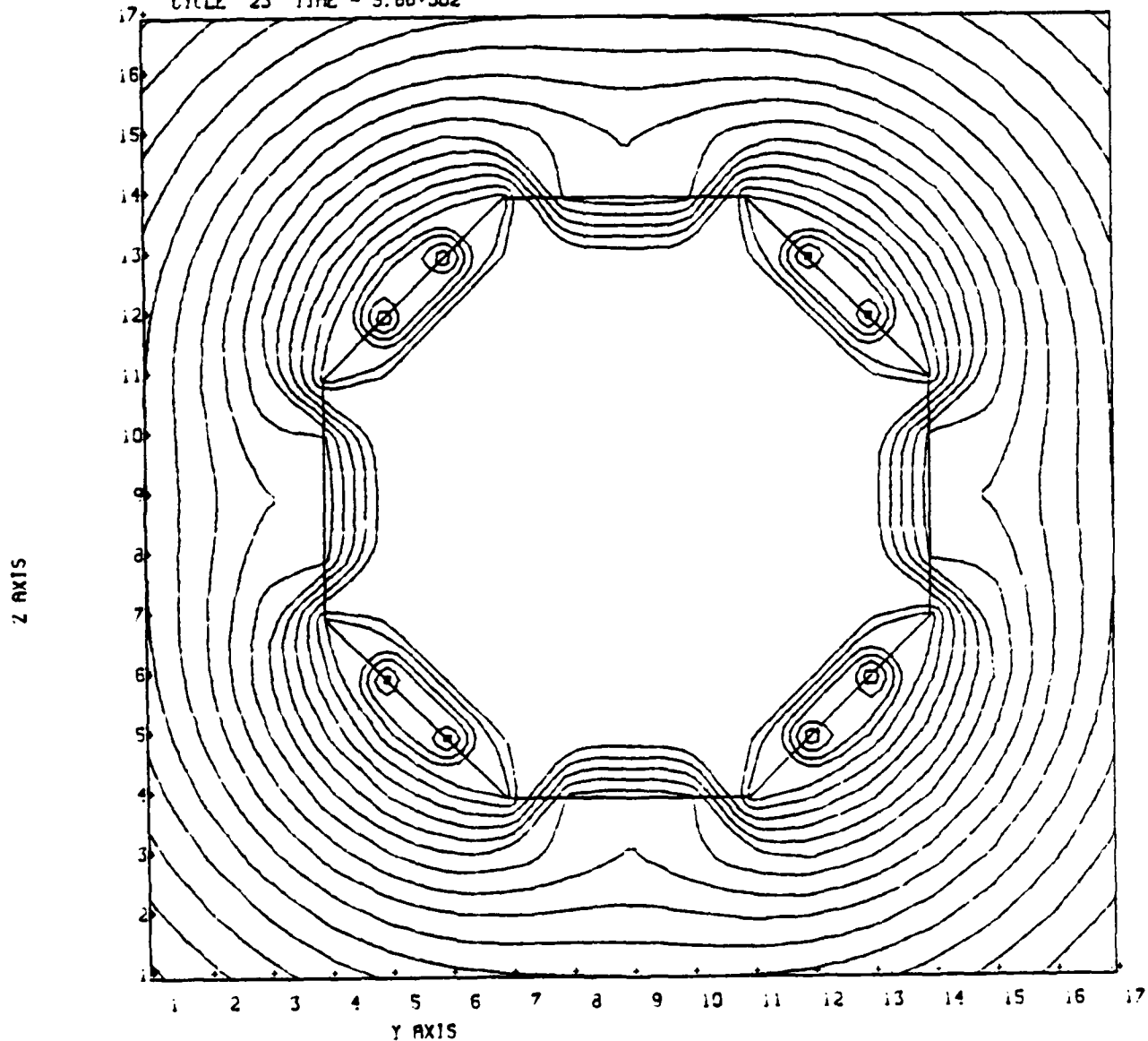
CYCLE 23 TIME - 5.86+002

Figure A-13.   Potential contours after ten minute exposure to
6 keV beams.

20

POTENTIAL CONTOURS ALONG THE X-Z PLANE OF Y - 9

ZMIN - -3.7611+003 ZMAX - -1.1940+003 DZ - 2.0000+002
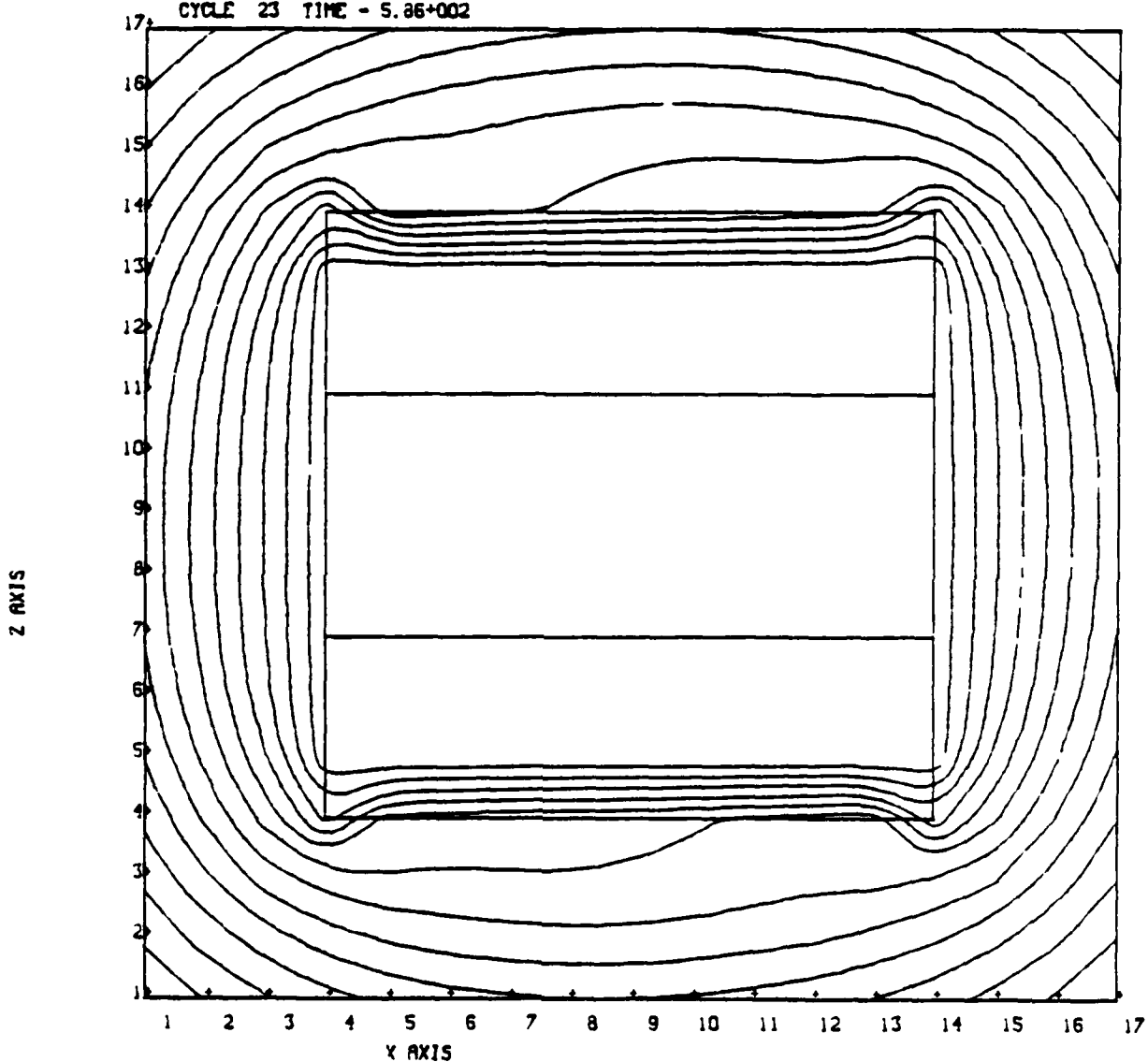
CYCLE 23 TIME - 5.86+002

Figure A-12. Potential contours after ten minute exposure to
6 keV beams. Regions of very low external
electric field near regions of high differential
charging are apparent. An object charged in
this manner will exhibit strong SGEMP enhance-
ment with high probability of synergistic sur-
face flashover.
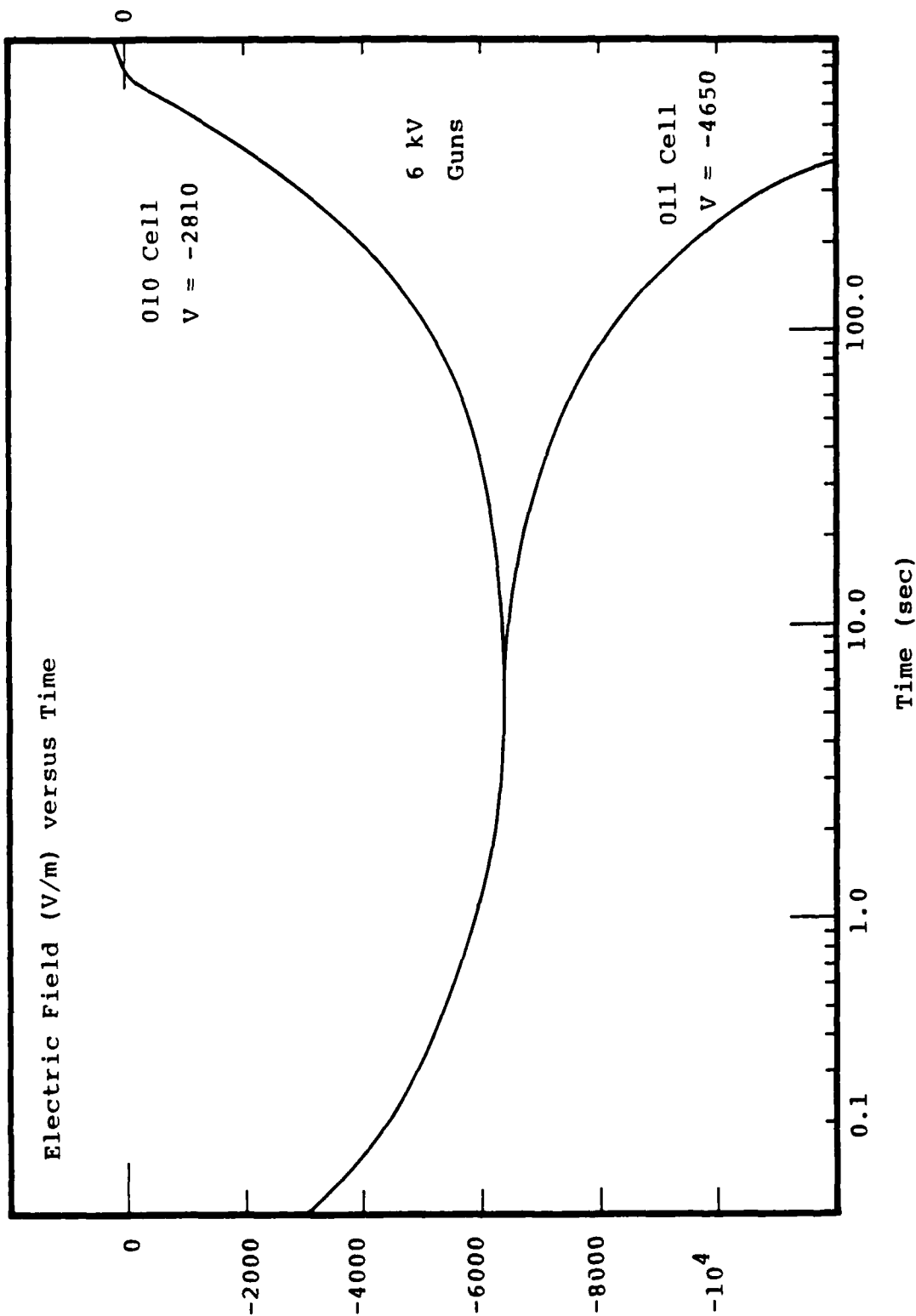
Figure A-11. Electric field for two neighboring cells near the object belly. After six minutes of exposure there is nearly two kilovolts of differential charging, and the electric field near the more positive cell changes sign. Its secondary electrons are now trapped. This is a likely region for a surface flashover discharge, either spontaneous or synergistically to an x-ray burst.
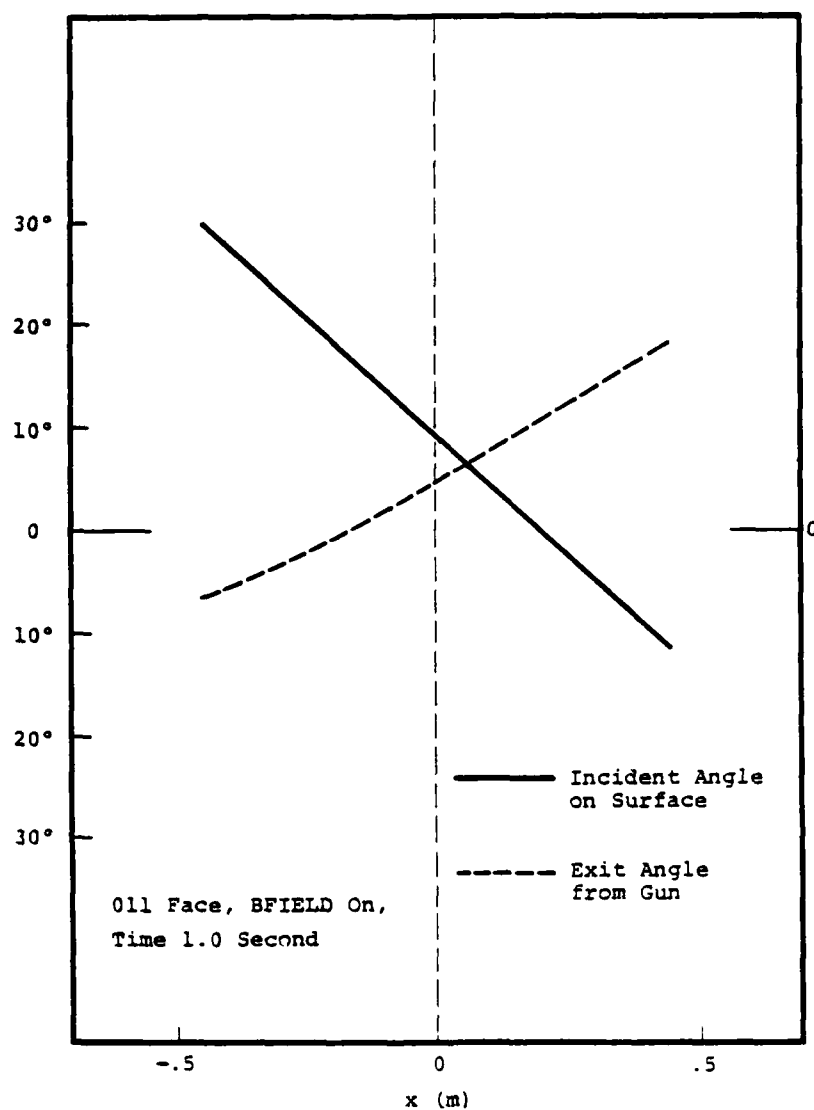
Figure A-10.   Resolution of paradox presented in previous figure. The dashed curve presents the angle (relative to gun axis) at which electrons must leave the gun to hit a given point on the object, taking into account magnetic deflection. The node of this curve, representing the densest part of the beam, is at x < 0. This is the main determinant of the early time flux curve, since secondary emission is fairly small. The solid curve represents the angle of incidence of electrons on the object surface. Its node (at x > 0) represents minimum secondary emission. The solid curve is the main determinant of the final fluxes and potentials.

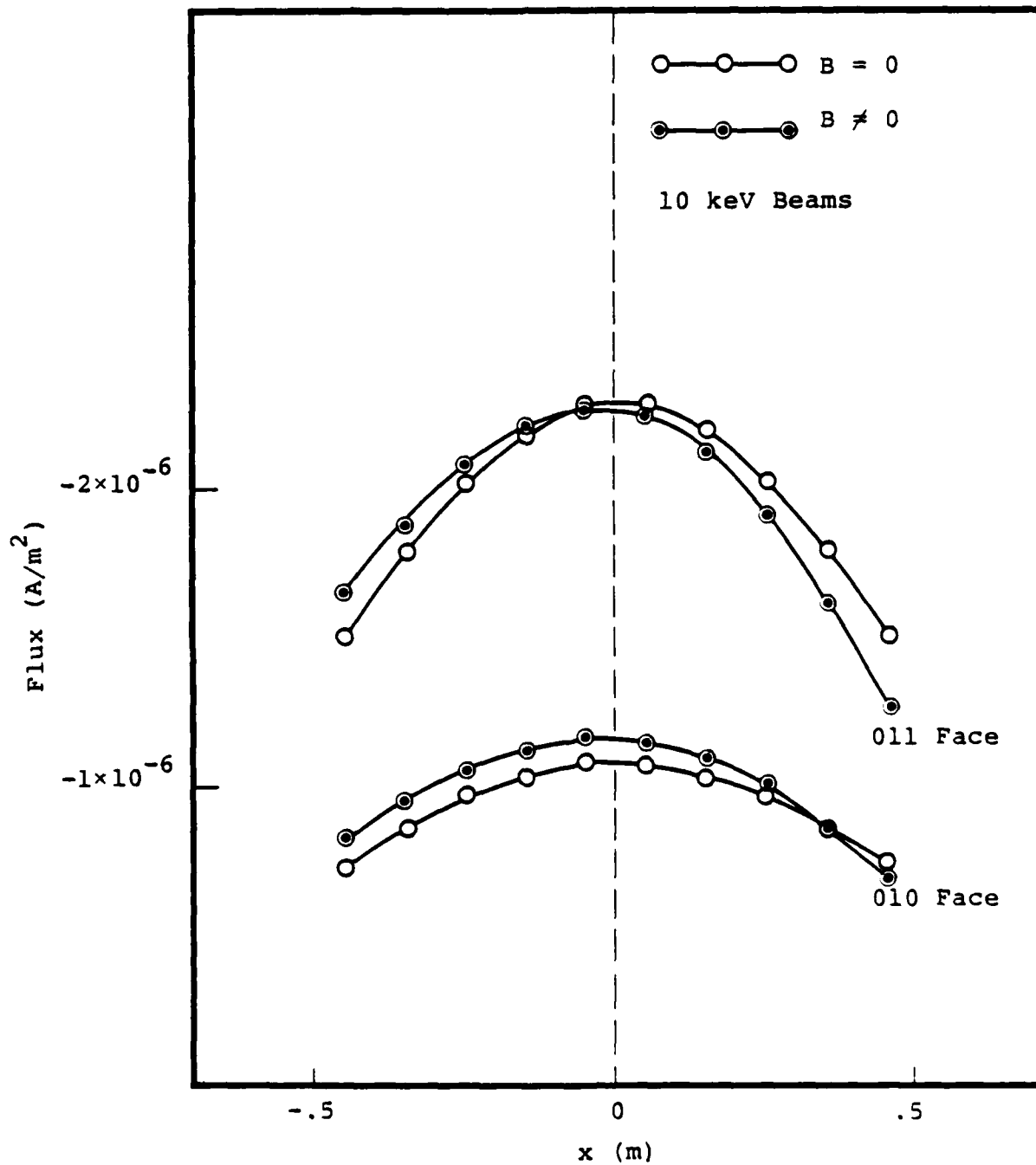Net Flux at t = 0.029 Seconds

Figure A-9. Fluxes as a function of height for the 10 keV cases at short time. This figure presents an apparent paradox, as the flux anisotropy is in the opposite sense from the final potentials.

16

POTENTIAL CONTOURS ALONG THE X-Z PLANE OF Y - 9

ZMIN - -3.6871+003 ZMAX - -1.1729+003 DZ - 2.0000+002
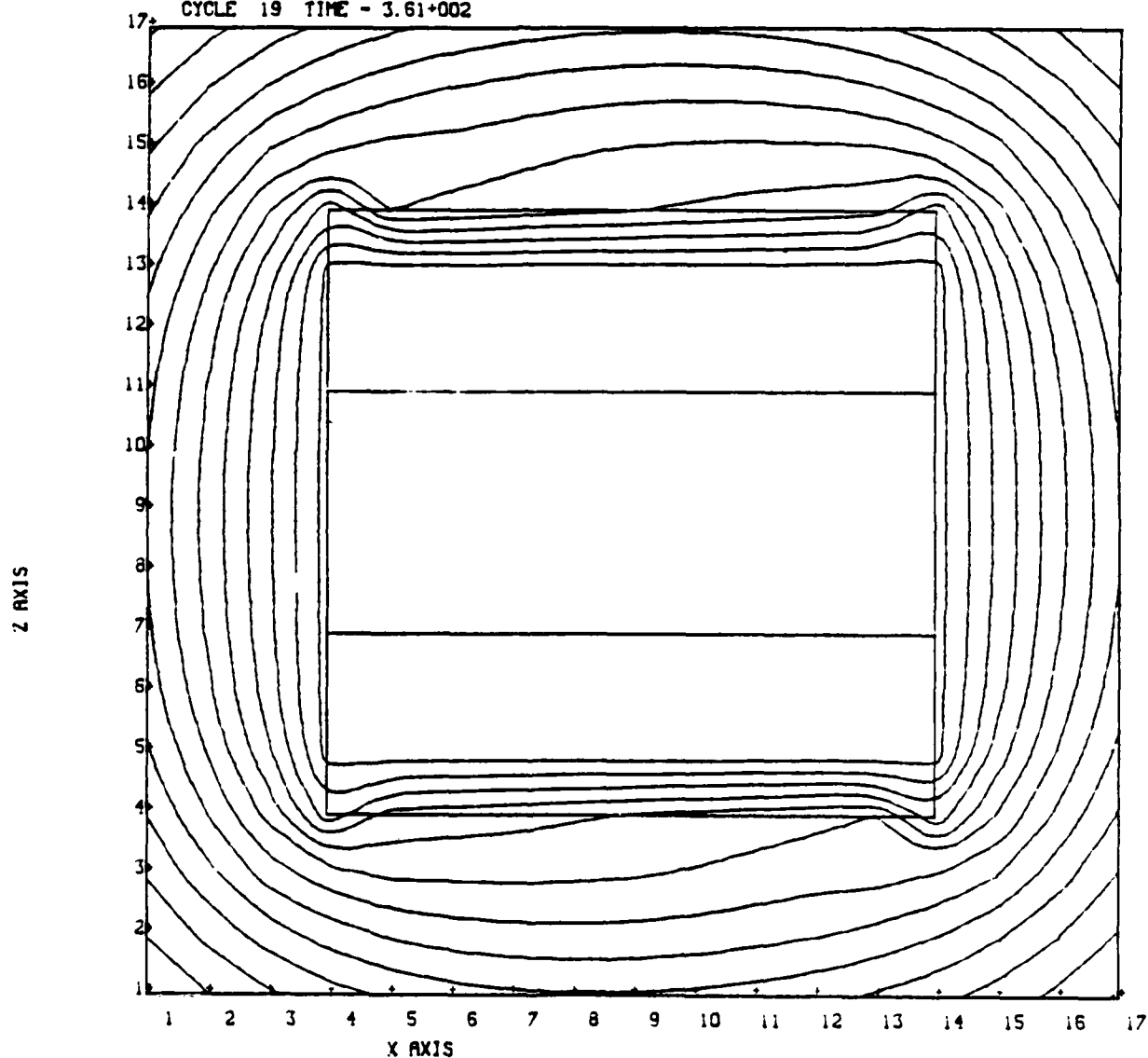
CYCLE 19 TIME - 3.61+002

Z AXIS

X AXIS

Figure A-8.   Side view of potential contours for the 6 keV
case.   The contours have the symmetry of the
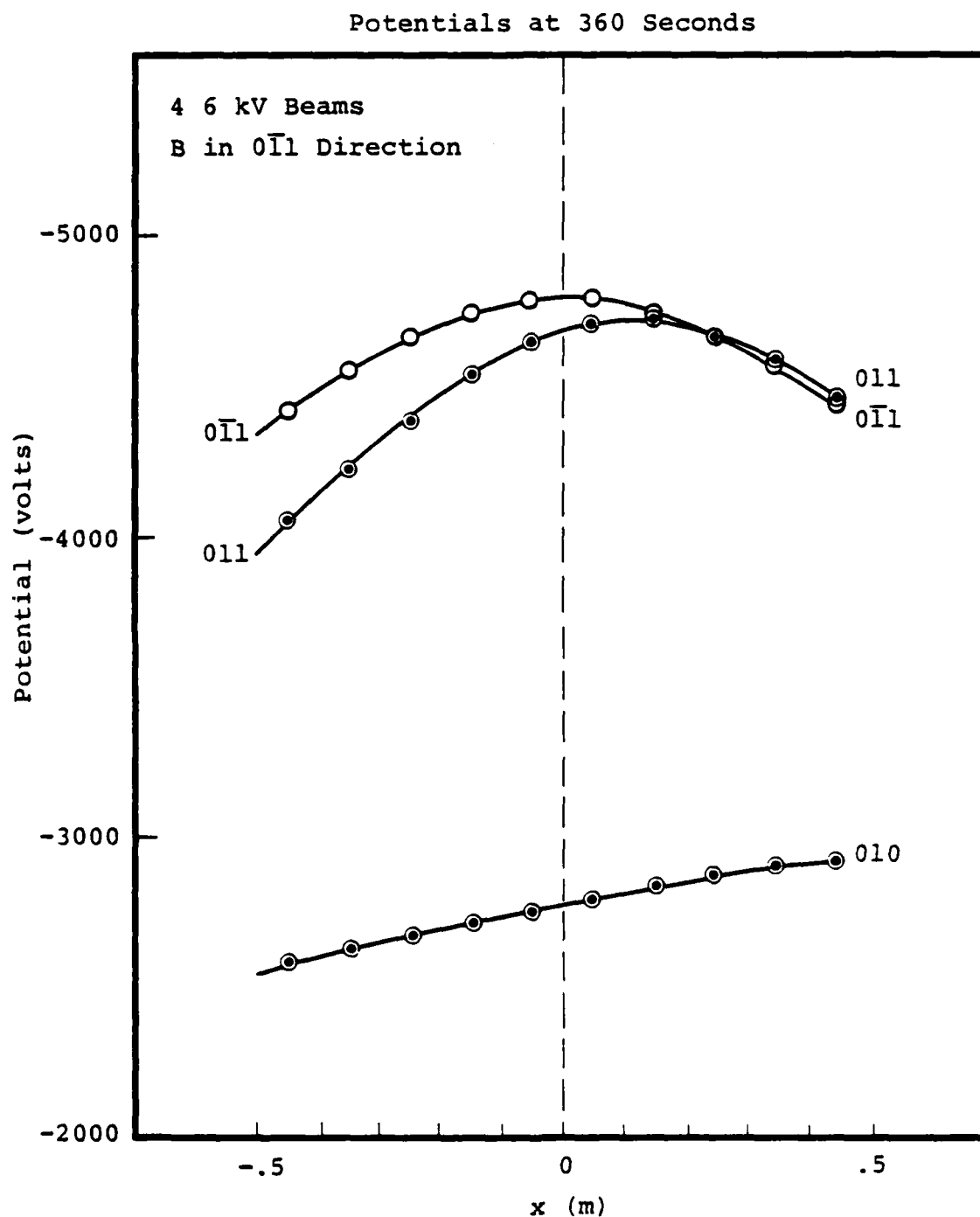magnetic field.

Figure A-7. Final (6 minute exposure) potentials for the 6 keV case. For lower energy the magnetic field has a greater effect.
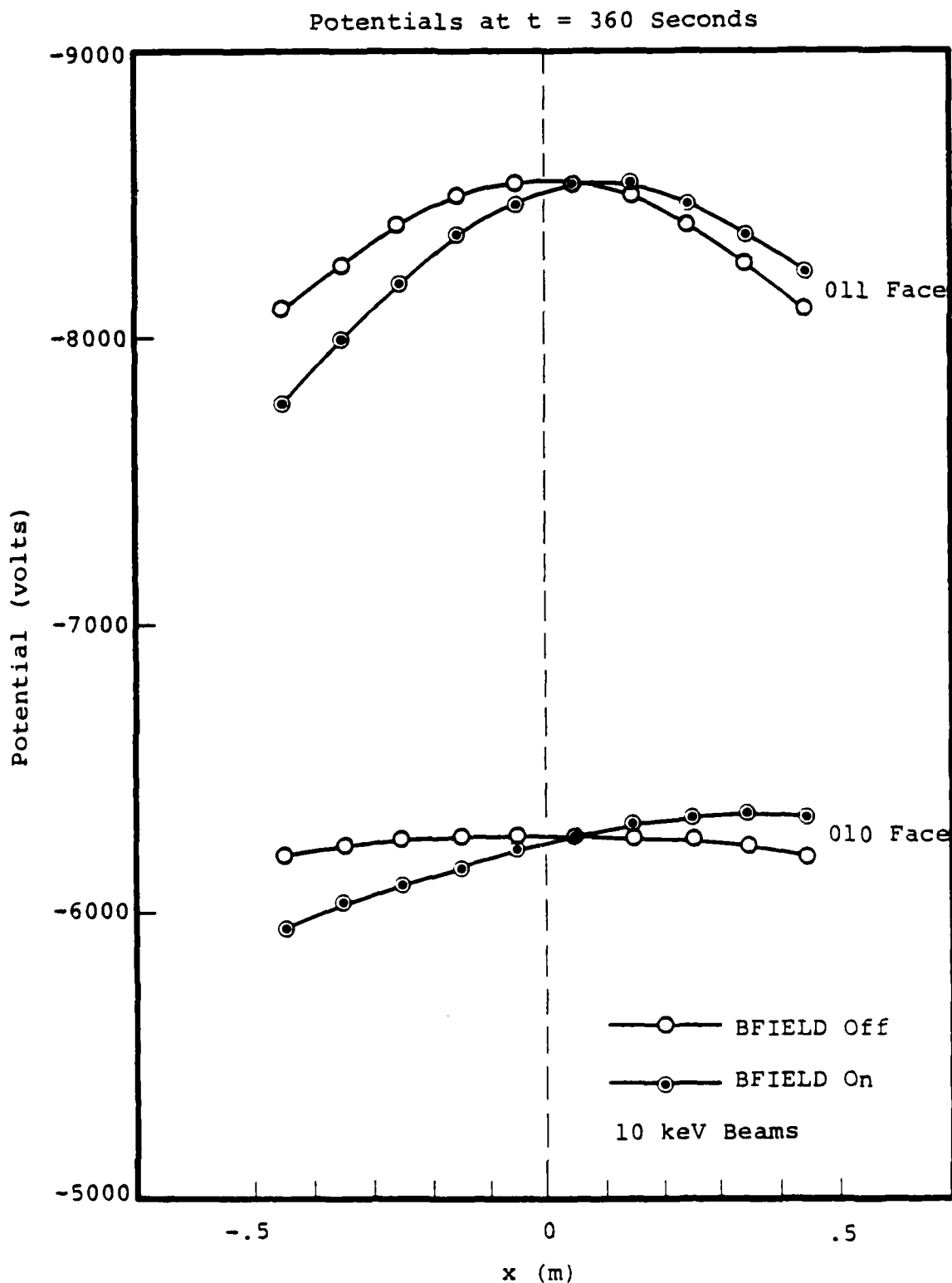
14

Figure A-6. Final (6 minute exposure) potentials for the 10 keV cases as a function of distance from the plane of the guns. The anisotropy caused by the magnetic field is apparent.
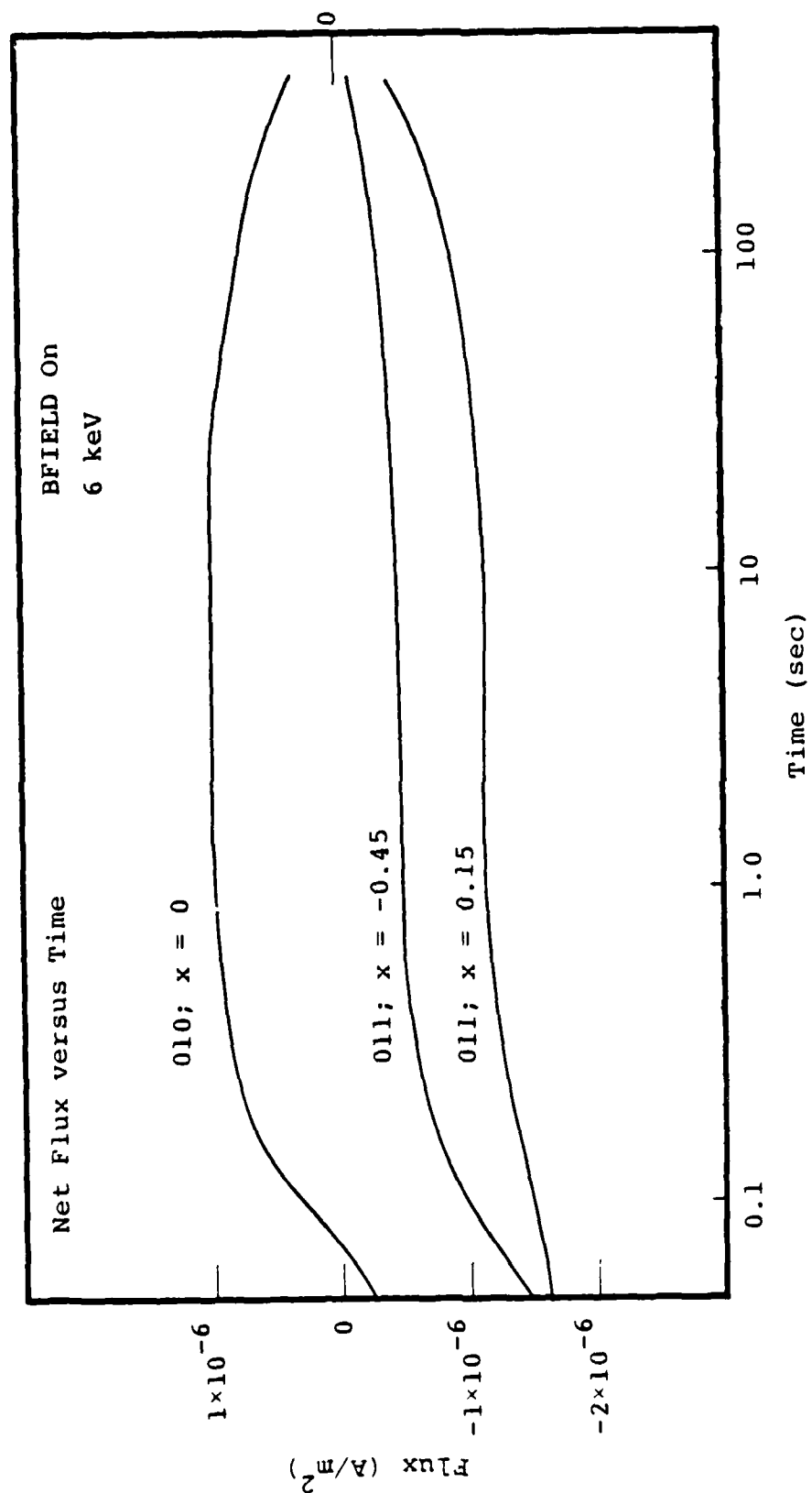
13

Figure A-5. Same as previous plot, but for the 6 keV case. Here we have drawn two curves to illustrate the range of fluxes on the 011 face.
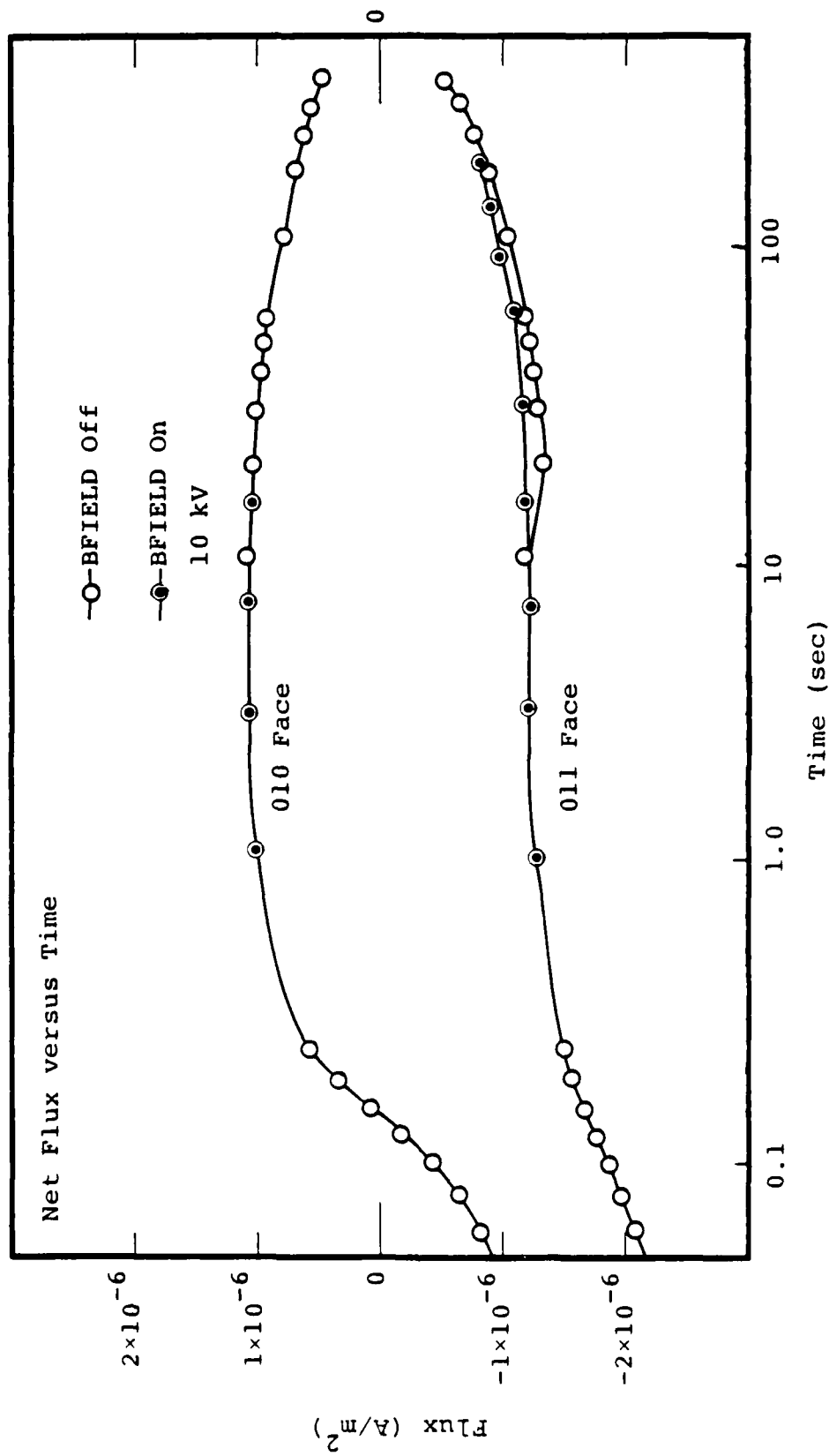
12

Figure A-4. Net flux to faces indicated versus time for the 10 keV runs, illustrating the same points as the previous potential plot. Note the reduction in differential flux as equilibrium is approached.

11

END

FILMED

10-85

DTIC